ORIGINAL ARTICLE

lajss.org© Latin American Journal of Solids and Structures

www.lajss.org

Quasi-Static and Dynamic Mechanical Properties of Reed Straw

Jiafeng Song[a], Guoyu Li[b*], Yansong Liu[c], Meng Zou[c]

[a]State Key Laboratory of Intelligent Green Vehicle and Mobility, Tsinghua University, Beijing, 100084, People's Republic of China. E-mail: iansongjiafeng@163.com
[b]School of Mechanical Engineering, Shanghai Dianji University, Shanghai, 201306, People's Republic of China. E-mail: ligy@sdju.edu.cn
[c]Key Laboratory for Bionics Engineering of Education Ministry, Jilin University, Changchun, 130022, People's Republic of China. E-mail: liuys23@mails.jlu.edu.cn, zoumeng@jlu.edu.cn

*Corresponding author

https://doi.org/10.1590/1679-78257991

Abstract

Slender reed straws in nature can withstand heavy weight of reed spikes and lateral wind force, and thus show good mechanical properties, especially compression resistance and shear resistance. In the paper, the quasi-static and dynamic mechanical properties of reed straws were studied. Three influencing factors of the straws were set according to the nodes (node-containing, node-free), location section (location 1, 2, 3, 4, 5), and moisture content (low, medium, high). The tensile strength of node-free reed straws with low moisture content ranged from 55.40 to 68.14 MPa at different locations. The axial compressive strength of node-containing straws was higher than that of node-free straws, and the influence of moisture content on the axial compressive strength was more obvious. The radial compressive strength of node-containing straws is 13.00 times higher than that of node-free straws in the corresponding part. The bending strength of straws gradually increases from the top to the root, and it is further enhanced with higher moisture content. The axial impact peak load of node-containing straws is up to 1.27 times that of node-free straws, and the axial impact peak load of straws with high moisture content is 1.40 times higher than that of straws with low moisture content in the corresponding part. The radial impact strength of reed straws gradually increases from the top to the root. In terms of bending impact strength, the impact toughness of reed straws ranges from 0.030 to 0.14 J·cm^2, and the specific energy absorption ranges from 1.09 to 4.35 J/kg. Because of the excellent mechanical properties, reed straws provide important material performance data for the engineering field and inspire the design of new engineering materials or structures by improving strength and reducing weight.

Keywords

Reed straws, node characteristics, water content, quasi-static mechanical strength, dynamic mechanical strength

Graphical Abstract

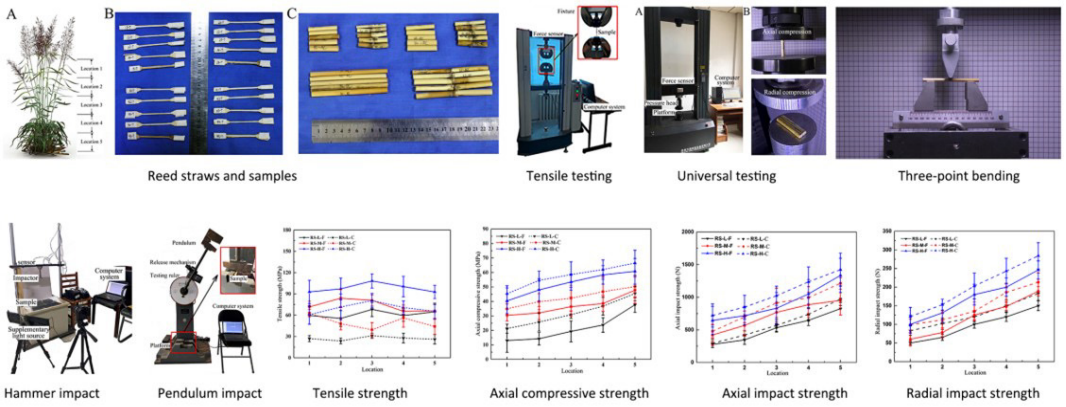

Received: January 17, 2024. In revised form: January 23, 2024. Accepted: January 30, 2024. Available online: February 05, 2024
https://doi.org/10.1590/1679-78257991

Latin American Journal of Solids and Structures. ISSN 1679-7825. Copyright © 2024. This is an Open Access article distributed under the terms of the Creative Commons Attribution License, which permits unrestricted use, distribution, and reproduction in any medium, provided the original work is properly cited.

1 INTRODUCTION

The structural comlocation of plant stalks can be categorized into two main types: node-containing and node-free (Stubbs et al. 2019; Yokozawa & Hara 1995). These node-containing structures are composite materials with anisotropy, comprising an outer layer, a columnar pith and nodes (Zou et al. 2015). Their lightweight and high-strength mechanical properties are issues worthy of analysis. Measuring the mechanical properties of straws offers insights for innovatively designing key components in crop harvesting machinery and optimizing the overall machine performance.

In terms of tensile properties, Yu measured the tensile stress, shear stress, tensile energy, and shear energy of corn straw upon destruction. The study identified the highest ultimate tensile stress as 69.3 MPa (Yu et al. 2014). Al-ZubeL focused on dry mature corn stalks, assessing their elastic modulus, and determining the accuracy and reliability of longitudinal compression and stretching (Al-Zube et al. 2018). Analyzing the tensile mechanical properties of straws not only reveals the material properties of stalk materials but also provides essential foundational data for stalk modeling (Kar et al. 2020; Özbek et al. 2009).

In terms of compressive characteristics, Stubbs used a finite element model to assist in determining the transverse Young modulus of the outer layer and pith of corn stalks, and the reliability of this method has been validated (Stubbs et al. 2019). Nona employed compression and relaxation models to characterize fiber materials, exploring the precision of the Faborode and Maxwell models in compression and the accuracy of the Maxwell and Peleg models in relaxation. The findings indicated that the Faborode model accurately portrays the compression curve, and for small deformations, the Maxwell model and the Faborode model exhibited similar effects (Nona et al. 2014). The compression mechanical properties of straws vary. Investigating these properties not only enhances essential data for stalk modeling but also offers guidance for the design and optimization of related machinery (Li et al. 2013; Amoah et al. 2012).

The shear mechanical properties of straws are closely related to the physical properties, such as moisture content (Gonzalez et al. 2015). Farman used a homemade shear box to compare the shear strength and specific shear energy between wheat and rice. As the loading rate rose, the shear strength, specific shear energy, and shear force of both wheat and rice increased (Chandio et al. 2013). Hoseinzadeh conducted shear experiments on the stalks of three wheat varieties at four moisture contents and three shear speeds. Wheat variety, moisture content and shear speed all significantly affected shear strength (Hoseinzadeh et al. 2009). Igathinathane conducted research on corn stalks with moisture content ranging from 15% to 20%. The experimental factors included cutting directions at 0°, 45°, and 90°. The cutting angle had a significant impact on the cutting force, with the shear force at 90° being 10 times greater than the shear force at 0° (Igathinathane et al. 2010). Studying the shear mechanical properties of straws can provide basic mechanical parameters for mechanical operations, such as stalk cutting and crushing (Tavakoli et al. 2008; Kumar et al. 2020).

Measuring the bending mechanical properties of straws can aid in understanding the lodging mechanism of crops and assist in the selection of suitable crop stalk cutters (Lundström et al. 2007; Leblicq et al. 2015). Robertson, using an enhanced three-point bending experiment method, demonstrated that the stalk shape significantly influenced the bending strength of the stalks (Robertson et al. 2017). A study on the deformation behavior of crops showed found that crop species, growth conditions, stalk diameter and wall thickness all significantly impacted the bending process, and the existence of the straw outer layer-pith structure improved the bending resistance of the stalks (Lundström et al. 2007). A cantilever bending experiment on sunflower stalks found the bending strength and elastic modulus of sunflower stalks differed among different parts, and the elastic modulus of the bottom stalks was larger (İnce et al. 2005).

Up to now, there has been limited in-depth research on the quasi-static and dynamic mechanical properties of reed stalks. As an cereal crop, reed stems hold significant potential applications in agriculture and ecology. Through a comprehensive mechanical analysis of reed stalks, this study aims to provide robust support for the further understanding and optimization of reed stalks. Combined with its natural lightweight and high strength, innovative materials can be designed and developed, especially those suitable for research in fields such as lightweight and efficient thin-walled tubes.

Reed (*Phragmites australis* (Cav.) *Trin. ex Steud*) stalks are upright, with 1-3 m in height and 1-4 cm in diameter, and have more than 20 nodes. The lightweight and high-strength properties make reed straws a suitable material for engineering research. In this paper, the quasi-static and dynamic mechanical properties of reed straws were studied, and mechanical data of the straws were collected, such as tensile strength, compressive strength, and bending strength. The quasi-static tensile, compression and bending characteristics of reed straws were analyzed through a tensile experimenter, universal experimenting machine and three-point bending experiment. The dynamic impact and bending characteristics of reed straws were analyzed through a drop hammer impact experimenter and a pendulum impact experimenter. Three influencing factors of the straws were set according to the nodes (node-containing, node-free), location section (location 1, 2, 3, 4, 5), and moisture content (low, medium, high). The influence of the nodes, moisture content and location section on the mechanical properties of the straws were analyzed.

2 MATERIALS AND METHODS

2.1 Samples

Reed straw samples were collected from Jiaozuo City, Henan Province, China. Only straws that were in good growth condition and free of diseases and insect pests were selected (Figure 1A). The straws had no obvious defects, skin damage, or cracks. To prevent moisture loss, the samples were sealed, and relevant mechanical property tests were conducted within 12 hours. The effects of location section, moisture content, and node characteristics on the mechanical properties of reed were analyzed. Each straw was divided into five sections, each 400 mm in length, from the top to the root: the upper part (location 1), upper-middle part (location 2), middle part (location 3), lower-middle part (location 4), and the lower part (location 5) (Figure 1B). The straws were divided into three control groups according to the moisture content: 40%-50% (fresh straws, high moisture content), 20%-30% (drying for 2 h, medium moisture content), and 5%-10% (drying for 8 hours, low moisture content). Based on the presence or absence of nodes, the straws were divided into two control groups: node-containing and node-free.

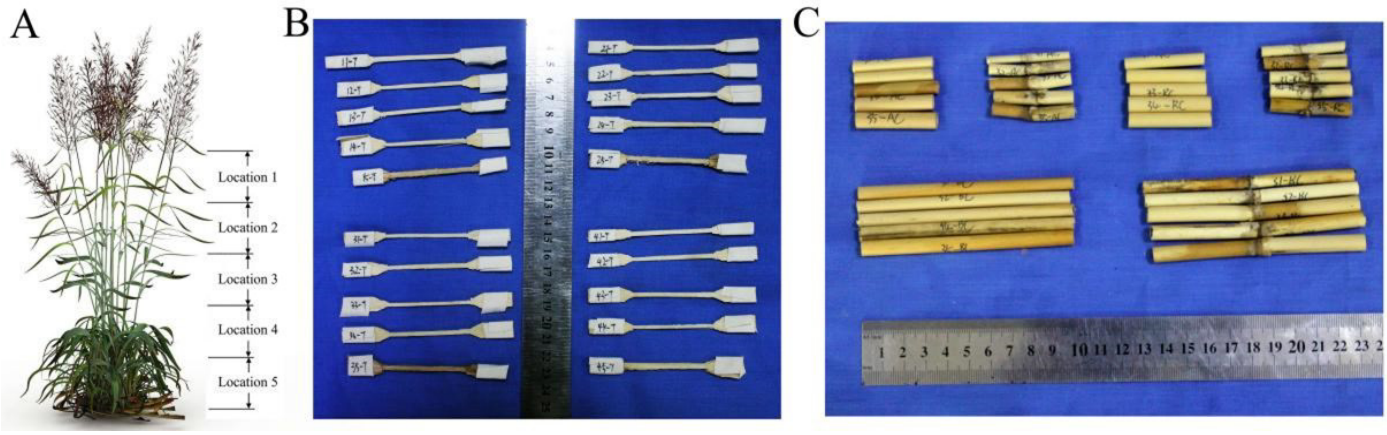

Figure 1 Reed straws and samples. (A) Reed, (B) Tensile sample, (C) Compression and bending samples.

2.2 Sample processing

Before the tensile test, the epidermal layer of each reed straw was made into a tensile sample (long strip) (Figure 1C). To avoid sliding during the stretching process, medical tape was wrapped at both ends of the sample. The samples were cut into cylindrical shapes during compression, bending and impact tests. Detailed dimensional standards of the samples were listed in Table 1. The samples were named as follows: reed straw (RL) - high moisture content (H)/medium moisture content (M)/low moisture content (L) - node-free (F)/node-containing (C). For example, RL-L-C represents the reed of node-containing sample with low moisture content.

Table 1 Sample specifications for mechanical tests

Sample type	Tensile sample	Compressive sample	Bending sample	Impact sample
Shape	long-stripped	cylindrical	cylindrical	cylindrical
Dimensions	length×width×thickness: 100.0×10.0×t mm^3	height×diameter: 40.0×d mm^2	height×diameter: 120.0×d mm^2	height×diameter: 40.0×d mm^2

2.3 Instruments

2.3.1 Tensile tester

The devices used in the tests include a WANCE-300 electronic universal material tester, a vernier caliper, and a steel ruler. The test devices were shown in Figure 2. The test environment temperature was 20 °C and the humidity was 70%. In this test, tensile stress was applied to the samples at a test speed of 5 mm/min. As the load increased, the tensile test was considered successful when the fracture points were not at both ends of the sample. To avoid breakage and slippage during the tensile test, a special wave-shaped chuck was used, and a layer of 2 mm thick rubber gasket was attached to the clamping part.

Based on the typical mechanical changing curve combined with the material mechanics equation (1), the tensile strength was calculated:

$$\sigma_{\max} = \frac{F_{\max}}{A} \tag{1}$$

where $\sigma_{\max}$ is the maximum tensile strength (MPa), $F_{\max}$ is the maximum load during the loading process (N), and A is the cross-sectional area of the sample (mm^2).

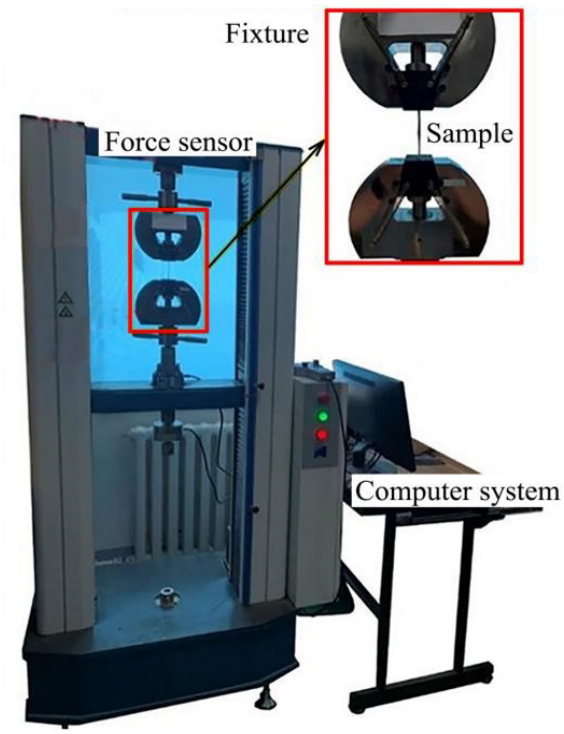

Figure 2 Tensile testing machine.

2.3.2 Universal tester

Axial and radial compression tests were conducted using a universal testing machine (Figure 3). During axial compression, the tested sample was placed vertically on the stage and compressed to 60% of its height. During radial compression, due to the small radial diameter, the sample was compressed to 50% of the sample diameter.

The load-displacement data collected during the longitudinal compression process were used to calculate the radial compressive strength through equation (2)::

$$\sigma_{jy} = \frac{3}{2}\left(\frac{F_{jy\max}}{2al_{jy}}\right) \tag{2}$$

where σ_{jy} is the radial compressive strength (MPa), $F_{jy\max}$ is the maximum radial pressure (N), and l_{jy} is the length of a radial compression sample (mm).

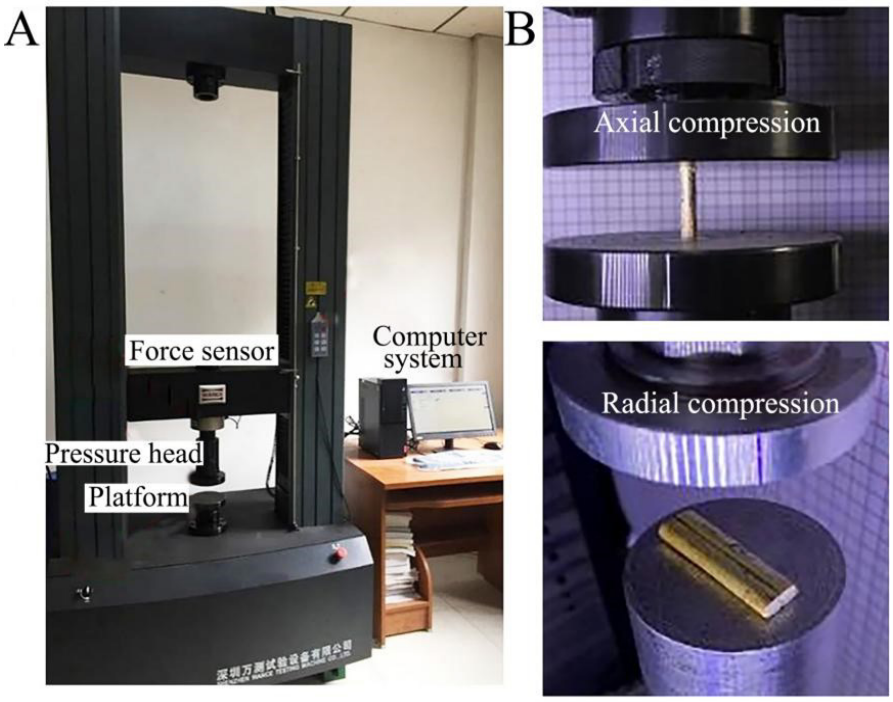

Figure 3 Universal testing machine.

2.3.3 Three-point bending test

The tested sample was placed horizontally on two supporting rollers. For the node-free straws, the compression loading point was located in the middle of the sample, and for the node-containing straws, the loading point was located on the node feature (Figure 4). The load-displacement curve of reed straws during three-point bending shows two stages: the elastic deformation stage and the failure stage. The bending strength of the straws was calculated using equation (3):

$$\sigma_{\omega} = \frac{8F_{\omega\max}l_{\omega}}{\pi(2b)^3} \tag{3}$$

where σ_{ω} is the bending strength (MPa), $F_{\omega\max}$ is the maximum bending force (N), and l_{ω} is the length of the straw bending sample (mm).

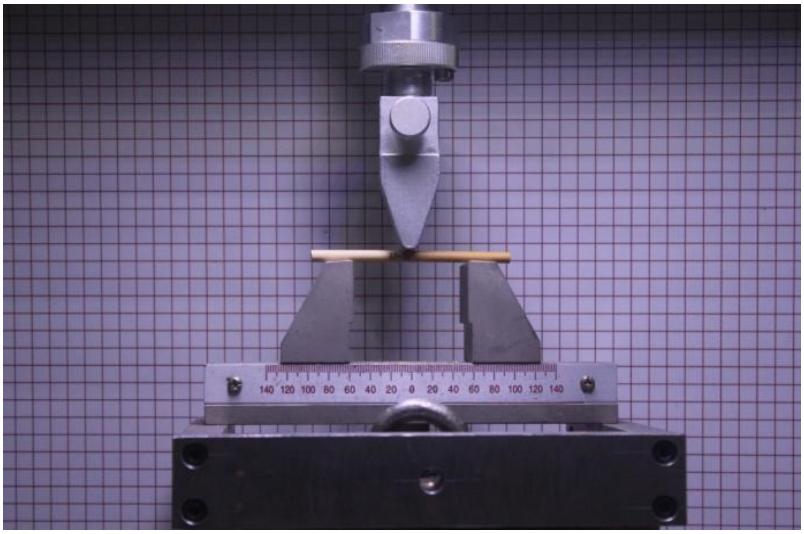

Figure 4 Three-point bending test.

2.3.4 Drop hammer impact tester

A self-developed small drop hammer impact tester was adopted (Figure 5). This system mainly includes steel hard ground, a calibration plate, an impactor, slide rails, an acceleration sensor, a data collector, a computer, a high-speed camera, and a supplementary light source. During the test, the sample was divided into two directions (axial impact and radial impact) and placed on the steel hard ground. The impactor weighed 8 kg and had a release height of 0.65 m. At a specified height, the impactor beam was released, allowing the impactor to fall freely and impact the sample. The acceleration sensor was used to record the changes in the impactor acceleration during the impact process. Simultaneously, the high-speed camera system recorded the displacement process of the impactor in relation to the calibration plate and documented the deformation and damage processes of the sample.

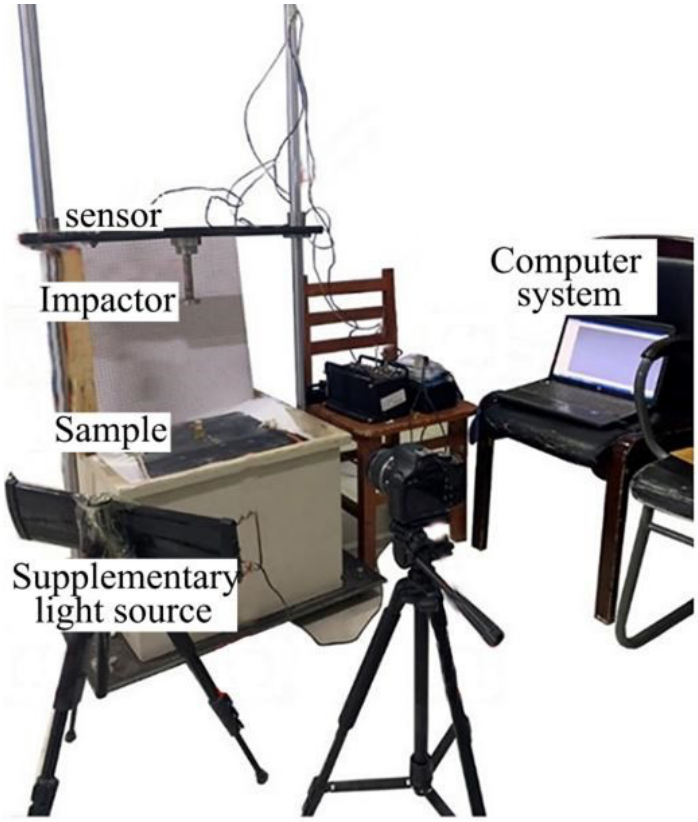

Figure 5 The drop hammer impact test system.

2.3.5 Pendulum impact tester

The standard pendulum impact testing system was shown in Figure 6. During the test, the sample was placed on the stage, and the pendulum was allowed to fall freely and swing at a given height. The mass of the pendulum was 13 kg. The impact energy was calculated using the pendulum's weight and the angular displacement before and after impact. Impact toughness is an important mechanical property that measures the impact resistance of a material and determines its brittleness and toughness. The impact toughness (J/cm2) was calculated using equation (4), and the impact energy was used for normalization to obtain the specific energy absorption (SEA):

$$a = \frac{A}{bh} \tag{4}$$

where A is the impact energy (J), b is the sample length (cm), and h is the sample width (cm).

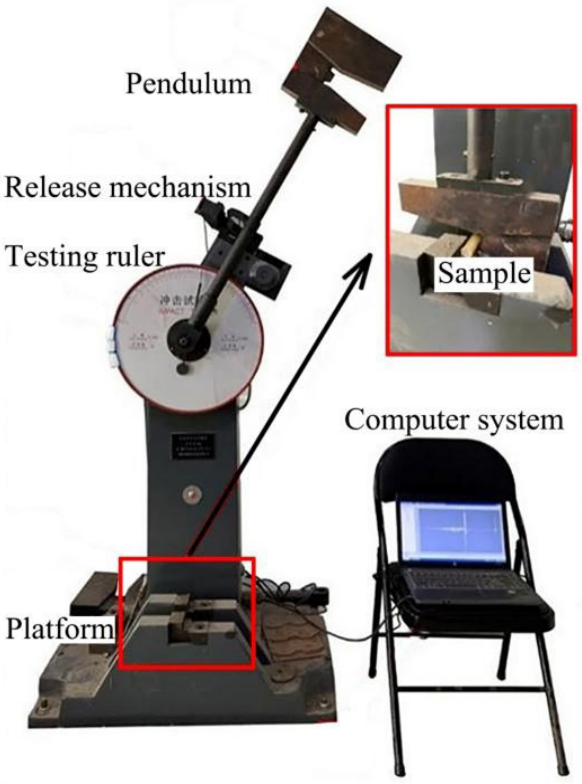

Figure 6 The pendulum impact test system.

3 RESULTS

3.1 Quasi-static tensile properties

During tensile tests, node-containing straws were more prone to break. This was attributed to the directional deviation of fibers at the nodes, leading to reduced strength along the grain direction. This observation highlights the directionality and high strength of fibers along the grain direction. Under all conditions, the minimum and maximum tensile strengths of reed straws were 23.74 and 100.38 MPa, respectively (Figure 7). The tensile strength of node-free straws is up to 2.48 times higher than that of node-containing straws in the corresponding section. Moreover, the tensile strength of samples with high moisture content is up to 4.36 times higher than that of samples in the corresponding section. The tensile strength of node-free straws is higher than that of node-containing samples. The tensile strength of node-free reed straws with low moisture content ranged from 55.40 to 68.14 MPa at different locations. The tensile strength of reed straws was significantly affected by moisture content and showed no correlation with the location section.

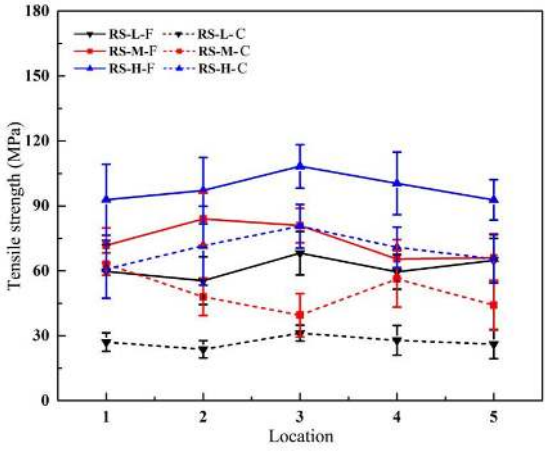

Figure 7 Tensile strength of node-containing and node-free straws at different locations and moisture contents.

3.2 Quasi-static compression strength

3.2.1 Axial compression strength

The failure modes of node-free straws and node-containing straws under axial compression load were shown in Figure 8. As the displacement increased, node-free straws were prone to complete rupture, while node-containing samples cracked evenly. The node features played a role in inhibiting the occurrence of cracks. Due to the hollow structure of the reeds and the lack of core support, the shell of the reed straws not only folds and deforms outwards, but also deforms inward.

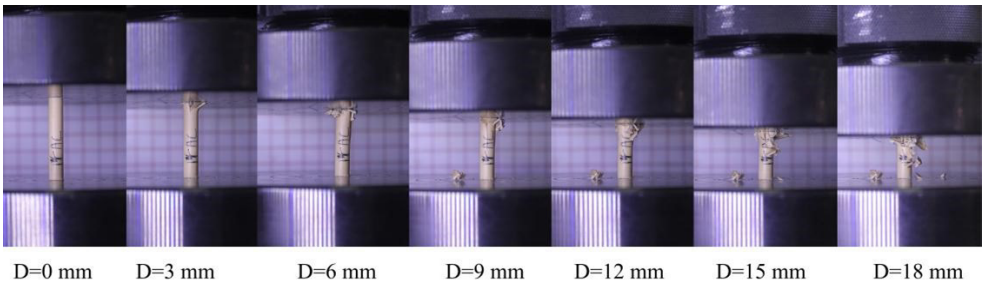

Figure 8 Failure mode of reed straws under axial compressive loading.

For reed straws, the minimum axial compressive strength is 13.00 MPa and the maximum is 66.51 MPa (Figure 9). The compressive strength of node-containing straws is 4.42 times higher than that of node-free straws in the corresponding part. The compressive strength of straws with high moisture content is 11.43 times higher than that of straws with low moisture content in the corresponding part. The axial compressive strength of reed straws was gradually enhanced from the top to the root. This phenomenon was more obvious especially when the moisture content was low. The axial compressive strength of node-containing straws was higher than that of node-free straws, and the influence of moisture content on the axial compressive strength was more obvious. The main reason is that when the moisture content is low, reed straws are more likely to break without the support and connection of the core.

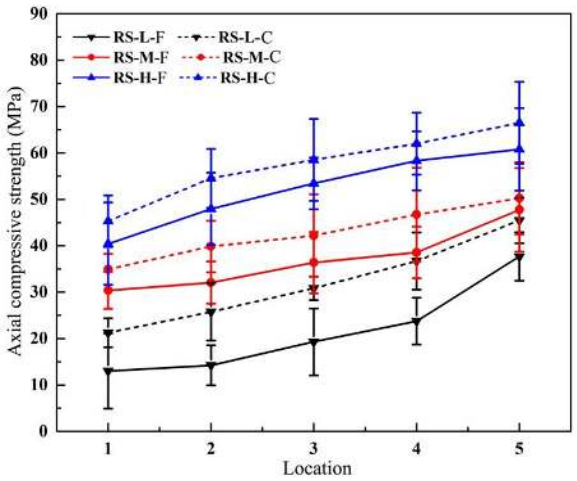

Figure 9 Axial compressive strength of node-containing and node-free reed straws at different locations and moisture contents.

3.2.2 Radial compression strength

The failure modes of the reed straw samples under radial compression load are shown in Figure 10. As the displacement increased, the straws gradually changed from a regular cylindrical shape to a flat shape along the radial direction. During radial compression, the outer layer of the node-free straws peeled off, while the node-containing straws were still connected after fracture, and the fracture at the nodes was suppressed to a certain extent.

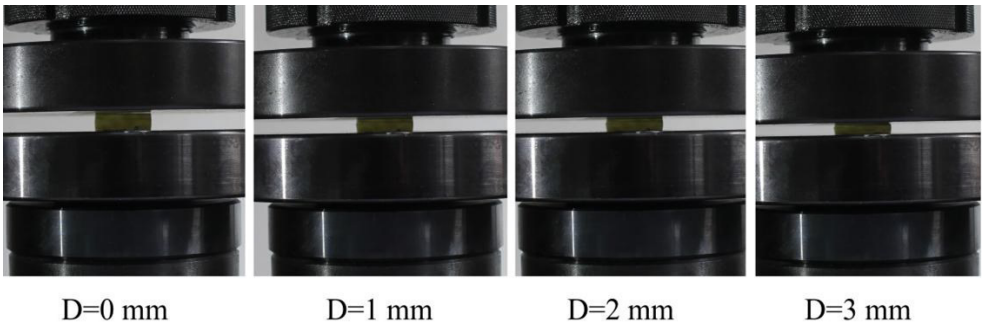

Figure 10 Failure mode of reed straws under radial compressive loading.

For reed straws, the minimum radial direction compressive strength is 0.06 MPa and the maximum is 1.62 MPa (Figure 11). The radial compressive strength of node-containing straws is 13 times higher than that of node-free straws in the corresponding part. The radial compressive strength of straws with high moisture content is 6.6 times higher than that of straws with low moisture content in the corresponding part. High moisture content and node characteristics significantly enhanced the radial compressive strength. At the same time, the compressive strength of the straws gradually increased from the top to the root.

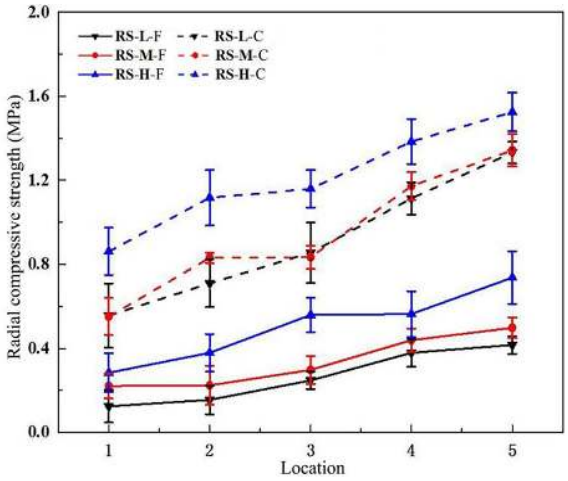

Figure 11 Radial compressive strength of node-containing straws and node-free straws at different locations and moisture contents.

3.3 Quasi-static bending strength

The three-point bending failure mode of reed straws is shown in Figure 12. When the load initially increased, the samples underwent elastic deformation. As the deformation continued to increase, yielding occurred until complete failure. Throughout the test, node-free samples essentially did not experience splitting, whereas most node-containing samples were prone to local failure or unilateral splitting. For node-free reed straws, local splitting was observed. In the case of node-containing reed straws, most samples exhibited local failure or unilateral splitting, but all splits occurred at the nodes, suggesting that nodes can inhibit splitting.

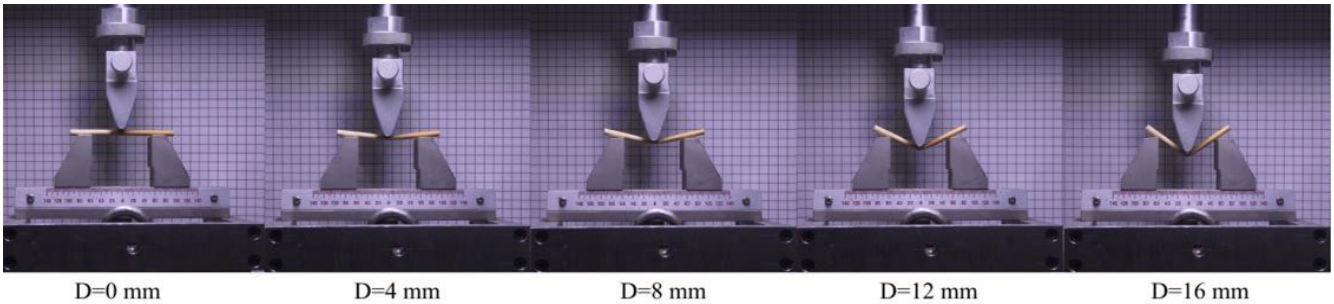

Figure 12 Bending failure mode of reed straws.

The minimum and maximum bending strengths of reed straws were 0.16 and 1.92 MPa respectively (Figure 13). The bending strength of node-free straws is up to 5.33 times higher than that of node-containing straws in the corresponding part, and the bending strength of samples with high moisture content is up to 7.34 times higher than that of samples with low moisture content in the corresponding part. The bending strength of straws gradually increased from the top to the root. The bending strength of straws with high moisture content and nodes was high, mainly because fractures were less likely to occur at node features with high moisture content.

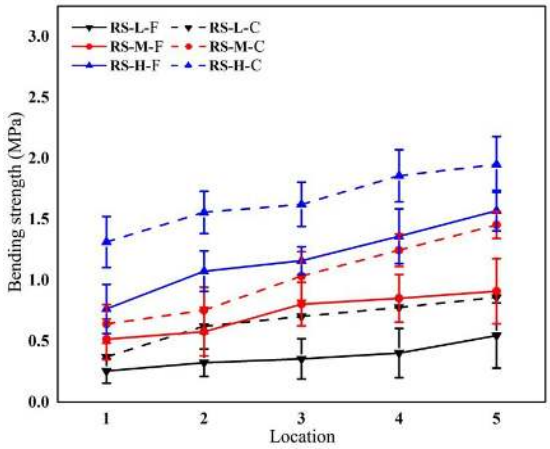

Figure 13 Bending strength of node-containing and node-free reed straws at different locations and moisture contents.

3.4 Dynamic impact strength

3.4.1 Axial impact strength

During the axial impact process, the deformation of the node-free straws occurred from top to bottom, and the bottom shell fibers folded. For node-containing samples, the node characteristics played an evident role in radial constraint. Folding occurred in the upper and lower parts of the nodes, and shell tearing was relatively uniform. The minimum axial impact peak load of reed straws is 277.00 N and the maximum is 1426.00 N (Figure 14). The axial impact peak load of node-containing straws is up to 1.27 times that of node-free straws in the corresponding part, and the axial impact peak load of straws with high moisture content is 1.40 times higher than that of straws with low moisture content in the corresponding part. In the axial impact test, the failure mode of reed straws was complete crushing, and the node characteristics of the straws inhibited the occurrence of cracks.

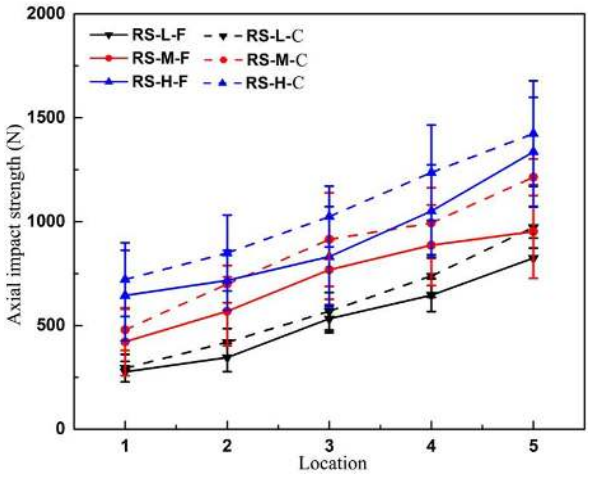

Figure 14 Axial impact strength of node-containing and node-free reed straws at different locations and moisture contents.

3.4.2 Radial impact strength

In the radial impact process, there was less difference in deformation, due to the smaller space for deformation. The minimum radial impact peak load of reed straws is 50.00 N and the maximum is 284.00 N (Figure 15). The radial

impact peak load of node-containing straws is up to 1.22 times that of node-free straws in the corresponding part, and the radial impact peak load of straws with high moisture content is 1.64 times that of straws with low moisture content in the corresponding part. The radial impact capacity of reed straws gradually increased from top to root, and the moisture content, along with node characteristics, enhanced the radial impact performance of the straws.

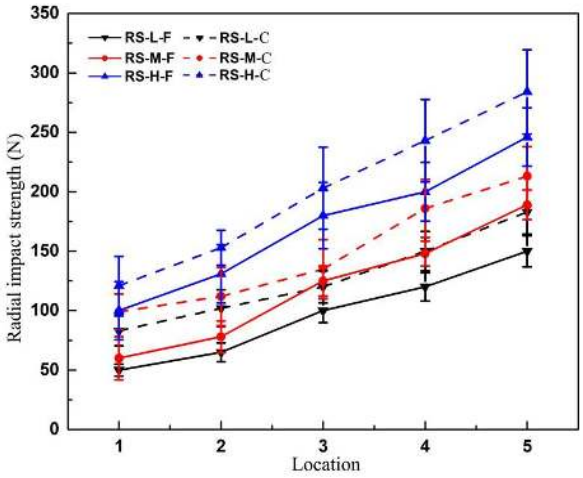

Figure 15 Radial impact strength of node-containing and node-free reed straws at different locations and moisture contents.

3.4.3 Bending impact strength

The impact toughness of reed straws ranges from 0.030 to 0.14 J·cm^2, and the specific energy absorption (SEA) varies from 1.09 to 4.35 J/kg (Figure 16). Compared with the node-free straws, the impact toughness and SEA of the node-containing straws in the corresponding parts are 2.44 and 1.18 times higher, respectively. Additionally, the impact toughness and SEA of samples with high moisture content are 4.80 and 2.19 times higher, respectively, than those of samples with low moisture content in the corresponding part. The impact toughness and SEA increased with the rise of moisture content. When the moisture content was low, the epidermal cells at the nodes lost more water, and the bonding force between the cell walls was smaller, making failure occur more easily. When the moisture content was high, the epidermal cells lost more water, and fibers at the nodes were well developed, providing strong impact resistance. The impact toughness of node-containing straws is significantly higher than that of node-free straws, which is mainly related to the changing pattern of straw diameter and wall thickness. The impact toughness gradually decreased from stalk top to root.

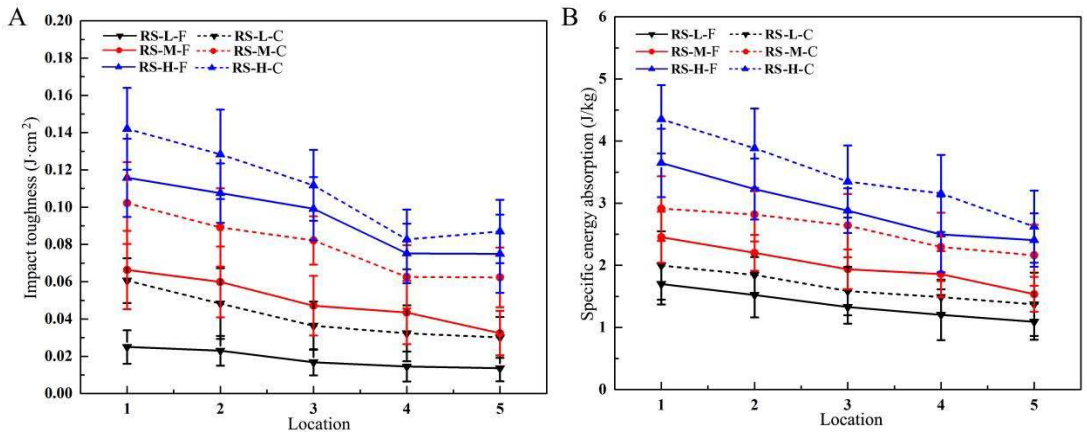

Figure 16 Impact bending resistance of reed straws. (A) Impact toughness of node straws and node-free straws at different locations and moisture contents, (B) Specific energy absorption of node straws and node-free straws at different locations and moisture contents.

4 CONCLUSION

In the paper, the quasi-static and dynamic mechanical properties of reed straws were studied, and mechanical data of the straws were collected. The quasi-static tensile, compressive and bending properties of reed straws were analyzed through a tensile tester, universal testing machine and three-point bending test, and the dynamic impact and bending properties of reed straws were analyzed with a drop hammer impact tester and a pendulum impact tester. Three influencing factors of the straws were set according to the nodes (node-containing, node-free), location section (locations 1, 2, 3, 4, 5), and moisture content (low, medium, high). The influence of the three factors on the mechanical properties of straws was analyzed.

The tensile strength of node-free straws is higher than that of node-containing straws. The tensile strength of node-free reed straws with low moisture content ranges from 55.40 to 68.14 MPa at different locations. The tensile strength of reed straws is significantly affected by moisture content and is unrelated to the location section. The axial compressive strength of node-containing straws is higher than that of node-free straws, and the effect of moisture content on the axial compressive strength is more obvious. The main reason is that when the moisture content is low, reed straws are more likely to break without the support and connection of the core. The radial compressive strength of node-containing straws is 13.00 times higher than that of node-free straws in the corresponding part, while the radial compressive strength of straws with high moisture content is 6.60 times higher than that of samples with low moisture content in the corresponding part. The bending strength of straw gradually increases from stalk top to root. The bending strength is enhanced with the rise of moisture content, and the strength of node-containing straws at high moisture content is significantly higher than that of node-free straws. The main reason is that fractures are less likely to occur at node features with high moisture content.

The axial impact peak load of node-containing straws is 1.27 times higher than that of node-free straws in the corresponding part, and the axial impact peak load of the samples with high moisture content is 1.40 times higher than that of samples with low moisture content in the corresponding part. Hence, the node characteristics of straws can inhibit the occurrence of cracks. In terms of radial impact strength, the load-bearing capacity of reed straws gradually increases from stalk top to root, and the moisture content and node characteristics play a certain role in enhancing the radial impact performance of the straws. In terms of bending impact strength, the impact toughness of reed straws ranges from 0.030 to 0.14 J·cm^2, and the SEA varies from 1.09 to 4.35 J/kg. Compared with the node-free straws, the impact toughness and SEA of the node-containing straws in the corresponding parts are 2.44 and 1.18 times higher, respectively. Additionally, the impact toughness and specific energy absorption of samples with high moisture content are 4.80 and 2.19 times higher, respectively, than those of samples with low moisture content in the corresponding part.

Reed straws have lightweight and high-strength mechanical properties, which provide potential for their wide applications in engineering. This study offers reference data for the development of innovative materials with excellent performance, which is especially important for such fields as lightweight and efficient thin-walled tubes. It also provides an important basis for the design of agricultural machinery and has practical application value for the innovative design and overall performance optimization of agricultural machinery.

Acknowledgements

This work was supported by the Special Project for the Project funded by China Postdoctoral Science Foundation (2022M721901),the Opening Project of the Key Laboratory of Bionic Engineering (Ministry of Education), Jilin University (K202208) and the Open Funding of Key Laboratory of Transportation Industry for Transport Vehicle Detection, Diagnosis and Maintenance Technology (JTZL2102).

Author's Contribuitions: Conceptualization, Jiafeng Song and Guoyu Li; Methodology, Jiafeng Song; Investigation, Guoyu Li, and Yansong Liu; Writing - original draft, Guoyu Li and Meng Zou; Writing - review & editing, Yansong Liu; Funding acquisition, Jiafeng Song; Resources, Jiafeng Song.

Editor: MARCÍLIO ALVES

References

Al-Zube L., Sun W., Robertson D., Cook D. (2018). The elastic modulus for maize stems. Plant Methods 14:1–12.

Amoah M., Appiah-Yeboahand J., Okai R. (2012). Characterization of physical and mechanical properties of branch, stem and root wood of Iroko and Emire tropical trees. Res. J. Appl. Sci. Eng. Technol. 4: 1755–1761.

Chandio F.A., Changying J., Tagar A.A., Mari I.A., Guangzhao T. (2013). Comparison of mechanical properties of wheat and rice straw influenced by loading rates. Afr. J. Biotechnol. 12: 1068–1077.

Gonzalez O., Gilbert B., Bailleres H., Guan H. (2015ICNSE). Shear mechanical properties of senile coconut palms at stem green tissue, in: Proceedings of 4th International Conference on Natural Sciences and Engineering, Kyoto Research Park, Japan, pp. 978–986.

Hoseinzadeh B., Esehaghbeygi A., Raghami N. (2009). Effect of moisture content, bevel angle and cutting speed on shearing energy of three wheat varieties. World Appl. Sci. J. 7: 1120–1123.

Igathinathane C., Womac A., Sokhansanj S. (2010). Corn stalk orientation effect on mechanical cutting. Biosyst. Eng. 107: 97–106.

İnce A, Uğurluay S., Güzel E., Özcan M. (2005). Bending and shearing characteristics of sunflower stalk residue. Biosyst. Eng. 92: 175–181.

Kar J., Rout A.K., Sutar A.K., Mohanty T. (2020). Study on static and dynamic mechanical properties of hybrid palm stalk fiber reinforced epoxy composites. Bioresources 15: 4249–4270.

Kumar A., Antil S.K., Rani V., Antil P., Jangra D., Kumar R., Pruncu C.I. (2020). Characterization on physical, mechanical, and morphological properties of Indian wheat crop. Sustainability 12: 2067.

Leblicq T., Vanmaercke S., Ramon H., Saeys W. (2015). Mechanical analysis of the bending behaviour of plant stems. Biosyst. Eng. 129: 87–99.

Li X., Wang S., Du G., Wu Z., Meng Y. (2013). Variation in physical and mechanical properties of hemp stalk fibers along height of stem. Ind. Crops Prod. 42: 344–348.

Lundström T., Heiz U., Stoffel M., Stöckli V. (2007). Fresh-wood bending: linking the mechanical and growth properties of a Norway spruce stem. Tree Physiol. 27: 1229–1241.

Nona K.D., Lenaerts B., Kayacan E., Saeys W. (2014). Bulk compression characteristics of straw and hay. Biosyst. Eng. 118: 194–202.

Özbek O., Seflek A., Carman K. (2009). Some mechanical properties of safflower stalk. Appl. Eng. Agric. 25: 619–625.

Robertson D.J., Julias M, Lee SY, Cook DD (2017). Maize stalk lodging: morphological determinants of stalk strength. Crop Sci. 57: 926–934.

Stubbs C.J., Sun W., Cook D.D. (2019). Measuring the transverse Young's modulus of maize rind and pith tissues. J. Biomech. 84: 113–120.

Tavakoli H., Mohtasebi S., Jafari A. (2008). Comparison of mechanical properties of wheat and barley straw, Agric. Eng. Int. 10: 1–9.

Yokozawa M., Hara T. (1995). Foliage profile, size structure and stem diameter-plant height relationship in crowded plant populations. Ann. Bot. 76: 271–285.

Yu M., Cannayen I., Hendrickson J., Sanderson M., Liebig M. (2014). Mechanical shear and tensile properties of selected biomass stems. Trans. ASABE 57: 1231–1242.

Zou M., Wei C., Li J., Xu S., Zhang X. (2015). The energy absorption of bamboo under dynamic axial loading. Thin Wall. Struct. 95: 255–261.